Metallostars

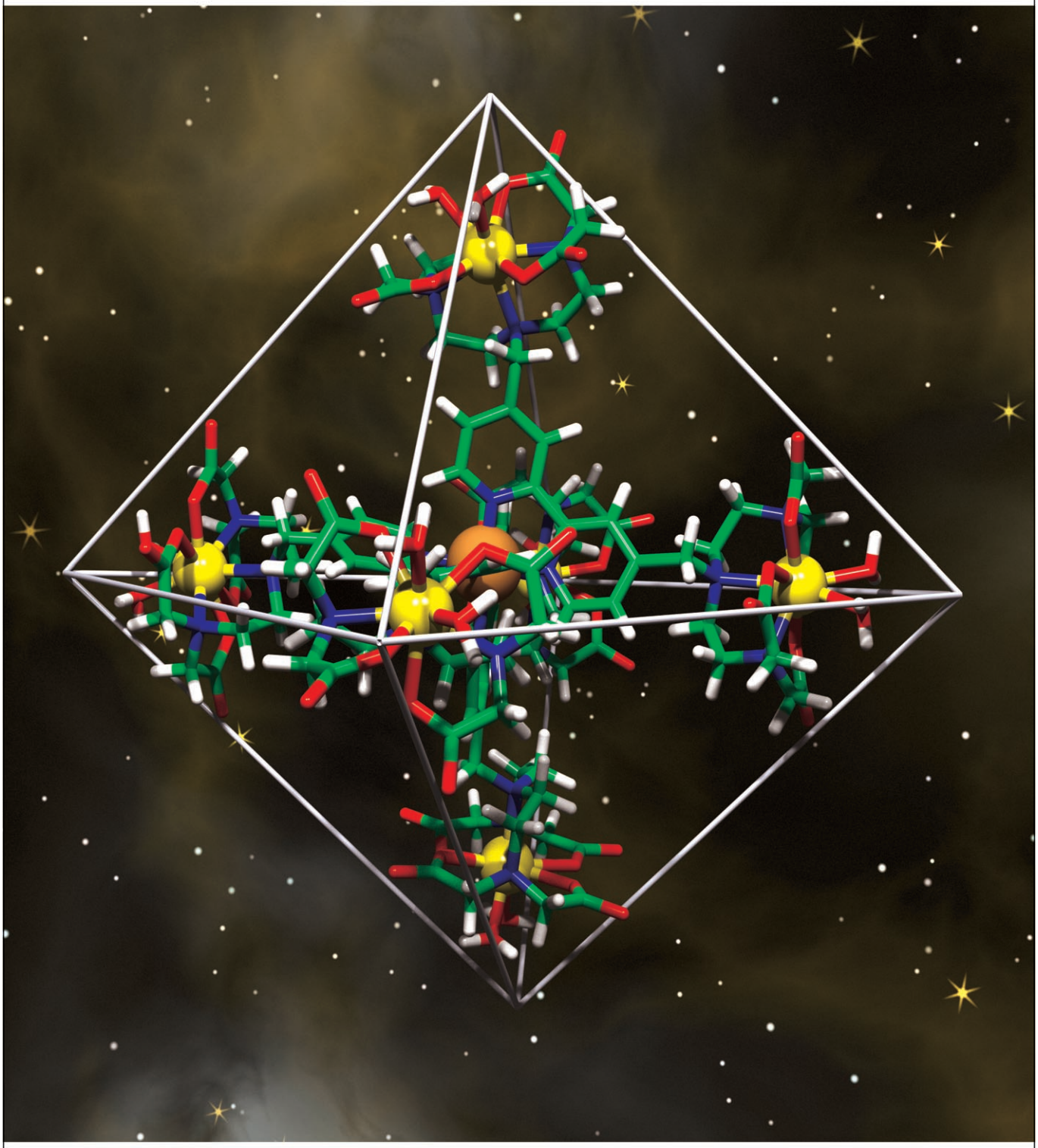

For more information see the following pages

CHEMISTRY
A EUROPEAN JOURNAL

DOI: 10.1002/chem.200500969

VIP

A Starburst-Shaped Heterometallic Compound Incorporating Six Densely Packed Gd^{3+} Ions

João Bruno Livramento, Angélique Sour, Alain Borel, André E. Merbach, and Éva Tóth*[a]

Abstract: The heterotritopic ligand $[bpy(DTTA)_2]^{8-}$ has two diethylenediamine-tetraacetate units for selective lanthanide(III) coordination and one bipyridine function for selective Fe^{II} coordination. In aqueous solution and in the presence of these metals, the ligand is capable of self-assembly to form a rigid supramolecular metallostar structure, $\{Fe[Gd_2bpy(DTTA)_2(H_2O)_4]_3\}^{4-}$. We report here the physicochemical characterization of the dinuclear complex $[Gd_2bpy(DTTA)_2(H_2O)_4]^{2-}$ and the metallostar $\{Fe[Gd_2bpy(DTTA)_2(H_2O)_4]_3\}^{4-}$ with regard to potential MRI contrast agent applications. A combination of pH potentiometry and ^1H NMR spectroscopy has been used to determine protonation constants for the ligand $[bpy(DTTA)_2]^{8-}$ and for the complexes $[Fe\{bpy(DTTA)_2\}_3]^{22-}$ and $[Y_2bpy(DTTA)_2]^{2-}$. In addition, stability constants have been measured for the dinuclear chelates $[M_2bpy(DTTA)_2]^{n-}$ formed with M = Gd^{3+} and Zn^{2+} ($\log K_{GdL} = 18.2$; $\log K_{ZnL} = 18.0$; $\log K_{ZnHL} = 3.4$). A multiple field, variable-temperature ^{17}O NMR and proton relaxivity study on $[Gd_2bpy(DTTA)_2(H_2O)_4]^{2-}$ and $\{Fe[Gd_2bpy(DTTA)_2(H_2O)_4]_3\}^{4-}$ yielded the parameters for water exchange and the rotational dynamics. The ^{17}O chemical shifts are indicative of bishydration of the lanthanide ion. The exchange rates of the two inner-sphere water molecules are very similar in the dinuclear $[Gd_2bpy(DTTA)_2(H_2O)_4]^{2-}$ and in the metallostar ($k_{ex}^{298} = 8.1 \pm 0.3 \times 10^6$ and $7.4 \pm 0.2 \times 10^6\ s^{-1}$, respectively), and are comparable to k_{ex}^{298} for similar Gd^{III} poly(amino carboxylates). The rotational dynamics of the metallostar has been described by means of the Lipari–Szabo approach, which involves separating global and local motions. The difference between the local and global rotational correlation times, $\tau_{lO}^{298} = 190 \pm 15$ ps and $\tau_{gO}^{298} = 930 \pm 50$ ps, respectively, shows that the metallostar is not completely rigid. However, the relatively high value of $S^2 = 0.60 \pm 0.04$, describing the restriction of the local motions with regard to the global one, points to a limited flexibility compared with previously reported macromolecules such as dendrimers. As a result of the two inner-sphere water molecules, with their near-optimal exchange rate, and the limited flexibility, the metallostar has a remarkable molar proton relaxivity, particularly at high magnetic fields ($r_1 = 33.2$ and $16.4\ mM^{-1}s^{-1}$ at 60 and 200 MHz, respectively, at 25 °C). It packs six efficiently relaxing Gd^{III} ions into a small molecular space, which leads, to the best of our knowledge, to the highest relaxivity per molecular mass ever reported for a Gd^{III} complex. The $[bpy(DTTA)_2]^{8-}$ ligand is also a prime candidate as a terminal ligand for constructing larger sized, Fe^{II} (or Ru^{II})-based metallostars or metallodendrimers loaded with Gd^{III} on the surface.

Keywords: heterometallic complexes · imaging agents · magnetic resonance imaging · relaxivity · self-assembly

Introduction

Since the introduction of magnetic resonance imaging (MRI) in clinical medicine in the early 1980s, there has been continuous interest in the development of more efficient, more tissue-specific, and lately, more responsive contrast agents.[1–3] These paramagnetic drugs, Gd^{III} complexes in the majority of cases, increase the image contrast by accelerating the relaxation of the surrounding water protons, and therefore contribute greatly to the excellent diagnostic performance of the magnetic resonance technique.

During the last two decades, much work has been devoted to the understanding of the mechanisms that govern the re-

[a] J. B. Livramento, Dr. A. Sour, Dr. A. Borel, Prof. A. E. Merbach, Dr. É. Tóth
Laboratoire de Chimie Inorganique et Bioinorganique
Ecole Polytechnique Fédérale de Lausanne, EPFL-BCH
1015 Lausanne (Switzerland)
Fax: (+41) 21-693-9875
E-mail: eva.jakabtoth@epfl.ch

Supporting information for this article (Equations used for the analysis of the ^{17}O NMR and NMRD data; variable-temperature, multiple field ^{17}O relaxation rates and chemical shifts measured for aqueous solutions of $[Gd_2bpy(DTTA)_2(H_2O)_4]^{2-}$ and $\{Fe[Gd_2bpy(DTTA)_2(H_2O)_4]_3\}^{4-}$ and for the diamagnetic reference; variable-temperature proton relaxivities as a function of the proton Larmor frequency) is available on the WWW under http://www.chemeurj.org/ or from the author.

laxation properties of Gd^{III} complexes. Particular attention has been paid to the design of new ligands allowing a simultaneous optimization of all parameters that influence efficiency. Proton relaxivity, commonly used to describe the efficacy of an MRI contrast agent, is defined as the longitudinal relaxation rate enhancement of bulk water protons induced by a 1 mmol L^{-1} concentration of Gd^{III}. The two main contributions to the relaxation process originate from an inner-sphere and an outer-sphere mechanism, the first being related to the exchange of the inner-sphere coordinated water, while the second arises from longer distance dipole–dipole interactions between Gd^{III} and bulk water protons. The inner-sphere proton relaxivity of a Gd^{III} complex is mainly dependent on the number of coordinated water molecules, their exchange rate with the bulk, the rotational motion of the molecule and that of the Gd-coordinated water proton vector in particular, as well as the electron spin relaxation of the paramagnetic center. The Solomon–Bloembergen–Morgan theory predicts maximum proton relaxivity when the water exchange is in a narrow, optimal range, and the rotation and electron spin relaxation are both slow.[4]

Recently, the water-exchange rate has been successfully tuned to optimal values in poly(amino carboxylate)[5–8] and other stable complexes of Gd^{III}.[9] In spite of the continuous work on the understanding of structure–mechanism relationships with regard to electron spin relaxation, it is not yet a straightforward matter to improve this factor through rational molecular design. As for rotational dynamics, from studies of diverse macromolecular contrast agents it became evident that rigid systems are indispensable for achieving maximum proton relaxivities. By detailed analysis of the rotational dynamics of dendrimers,[10,11] micelles,[12,13] and linear polymers[14,15] by means of the Lipari–Szabo approach,[16] it has been unambiguously proved that these macromolecular systems possess a significant degree of internal flexibility, which is either inherent to the macromolecule itself (linear polymers) or originates from the linker that connects the Gd^{III} chelate to the large molecule. In this respect, heterometallic self-assembled structures with a well-defined, rigid topology may represent a promising approach. Given their increased molar relaxivity resulting from the slow rotation and rigidity, along with the numerous Gd^{III} centers within one molecule, self-assemblies can be particularly beneficial to concentrate relaxivity into a small molecular space. In certain emerging applications of MRI, such as cell imaging, biological constraints seriously limit the amount of contrast agent deliverable into one cell without destroying it. Consequently, agents with many efficiently relaxing paramagnetic centers confined into a small space are advantageous compared to large macromolecules with few Gd^{III} centers. Additionally, the presence of different metals within the same molecule opens new perspectives towards multimodal contrast agents: the paramagnetic Gd^{III} can be exploited as an MRI probe, while another metal, such as Ru^{II}, also integral to the self-assembly, might behave as a fluorescent probe.

The first self-assembled heterometallic system was reported by Desreux et al.;[17] they synthesized a phenanthroline derivative of Gd(DO3A) that self-assembled with Fe^{II} to give a tetranuclear $FeGd_3$ entity (Scheme 1). This system was proposed as a contrast agent, the relaxivity of which is responsive to Fe^{II} concentration; however, no results have since been published in this direction. Recently, we reported a poly(amino carboxylate)-functionalized terpyridine ligand $(tpy\text{-}DTTA)^{4-}$ with distinct binding sites for Fe^{II} and Gd^{III}.[18,19] In aqueous solution and in the presence of these metals, the ligand self-assembles to form a rigid supramolecular structure, $\{Fe^{II}[Gd(tpy\text{-}DTTA)(H_2O)_2]_2\}$ (Scheme 1). In the heteroditopic ligand $(tpy\text{-}DTTA)^{4-}$, the central amine

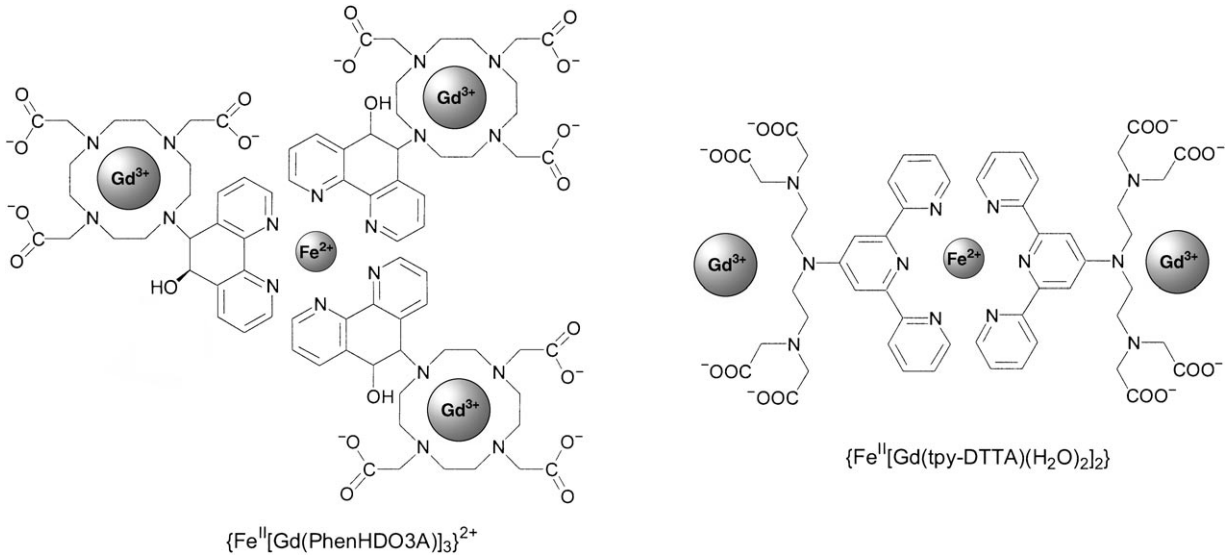

Scheme 1. Self-assembling systems previously studied in the context of MRI contrast agents.[17,19]

nitrogen of the Gd^{III}-binding poly(amino carboxylate) unit ($DTTA^{4-}$) is directly linked to the Fe^{II}-binding terpyridine part. This design efficiently eliminated internal flexibility, and largely contributed to the remarkable rigidity of the self-assembled molecule. Unfortunately, direct linkage of the aromatic ring to the amine nitrogen reduces the basicity of the amine, resulting in a large decrease in the thermodynamic stability of the Gd^{III} complex. The p*Gd* value of $\{Fe^{II}[Gd(tpy\text{-}DTTA)(H_2O)_2]_2\}$ (p*Gd* = 10.6 for pH 7.4, c_{Gd} = 1 μM, c_L = 10 μM) is several units lower than those of marketed contrast agents and precludes any biological application (p*Gd* is defined as the negative logarithm of the free metal ion concentration). Moreover, the neutral $\{Fe^{II}[Gd(tpy\text{-}DTTA)(H_2O)_2]_2\}$ complex was found to have limited solubility in water.

To circumvent the problem of low stability and solubility, we synthesized a novel, heterotritopic ligand, $H_8bpy(DTTA)_2$, possessing a 2,2′-bipyridine moiety for specific Fe^{II} binding and two poly(amino carboxylates) for Gd^{III} binding (Scheme 2). In a preliminary communication,[20] we reported that the ligand self-assembles with Fe^{II} and Gd^{III} to form a metallostar structure, $\{Fe[Gd_2bpy(DTTA)_2(H_2O)_4]_3\}^{4-}$. Metallostars are by definition first-generation metallodendrimers.[21] Usually, only compounds having a core connectivity of three or greater are considered, which excludes topologically linear dinuclear and trinuclear systems. The ligand $H_8bpy(DTTA)_2$ was designed by considering the following features. First, the Gd^{III} binding site, which is the same poly(amino carboxylate) chelating unit as in the previously described $TTAHA^{6-}$ (Scheme 2),[22] was chosen to guarantee sufficient thermodynamic stability, of fundamental concern for in vivo safety, and a near-optimal water-exchange rate. The two inner-sphere water molecules in the Gd^{III} complex double the inner-sphere contribution to relaxivity. Fe^{II} can accommodate three strongly coordinating 2,2′-bipyridine units, which increases to six the number of Gd^{III} centers on one iron core. The accumulation of six Gd^{III} centers in a small space represents a clear advantage over $\{Fe^{II}[Gd(tpy\text{-}DTTA)(H_2O)_2]_2\}$. Moreover, the negative charge of $\{Fe[Gd_2bpy(DTTA)_2(H_2O)_4]_3\}^{4-}$ ensures high water solubility, which is problematic for the neutral $\{Fe^{II}[Gd(tpy\text{-}DTTA)(H_2O)_2]_2\}$. The linking between the Fe^{II}

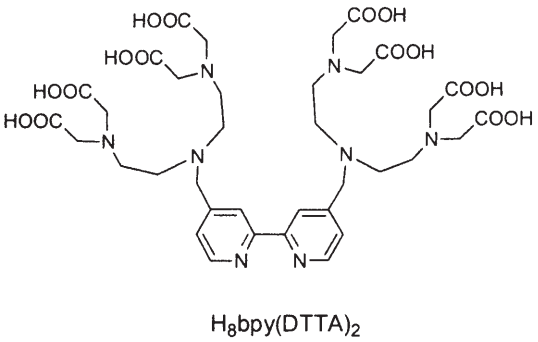

$H_8bpy(DTTA)_2$

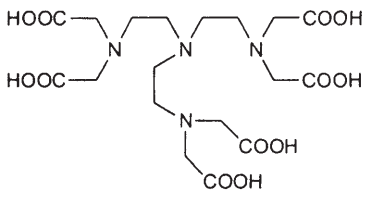

H_6TTAHA

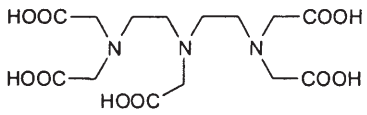

H_5DTPA

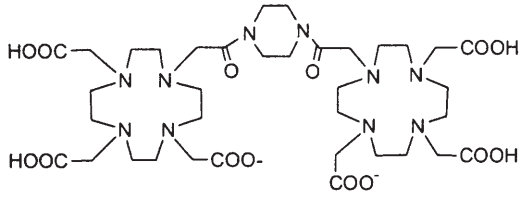

$H_6pip(DO3A)_2$

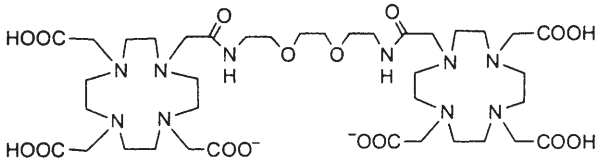

$H_6bisoxa(DO3A)_2$

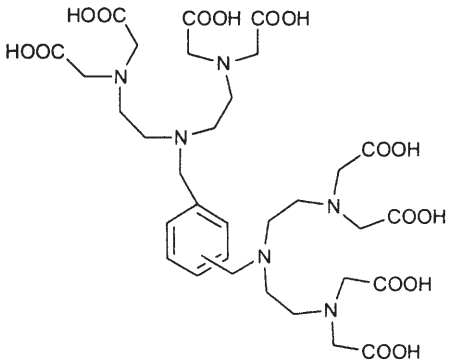

$H_8p,mX(DTTA)_2$

Scheme 2. Structures of ligands discussed in the text.

and Gd^{III} binding sites is designed to minimize internal flexibility that might reduce the relaxivity gain achieved by the increased molecular size.

Herein, we report a multiple field, variable-temperature ^{17}O NMR and NMRD study on both the dinuclear $[Gd_2bpy(DTTA)_2(H_2O)_4]^{2-}$ complex and the $\{Fe[Gd_2bpy(DTTA)_2(H_2O)_4]_3\}^{4-}$ metallostar, which has allowed us to define parameters for the water exchange and rotational dynamics. Furthermore, pH-potentiometry has been used to determine the protonation constants of the ligand, as well as the thermodynamic stability constants of the Gd^{III} and Zn^{II} complexes. In addition, relaxometric assays have been performed to assess the stability of the metallostar under biologically relevant conditions.

Results and Discussion

We have reported the ligand synthesis in a preliminary communication.[20] The dinuclear complex $[Gd_2bpy(DTTA)_2(H_2O)_4]^{2-}$ is prepared by mixing the ligand and Gd^{3+} in a 1:2 molar ratio at pH 6. The metallostar $\{Fe[Gd_2bpy(DTTA)_2(H_2O)_4]_3\}^{4-}$ forms instantaneously on adding Fe^{2+} to a solution of $[Gd_2bpy(DTTA)_2(H_2O)_4]^{2-}$, as indicated by the appearance of an intense red color. Since the formation of the metallostar from the dinuclear complex results in a remarkable increase in proton relaxivity, it can be conveniently followed either by relaxometry or by spectrophotometry.[20] Proton relaxivity measurements indicated that the metallostar is formed exclusively in a 1:3 $Fe:Gd_2L$ stoichiometry, as expected for an Fe^{II}-bpy complex. On adding increasing amounts of Fe^{II} to a solution of $[Gd_2bpy(DTTA)_2(H_2O)_4]^{2-}$, the relaxivity continuously increases until the $Fe^{II}/[Gd_2bpy(DTTA)_2(H_2O)_4]^{2-}$ molar ratio reaches 1:3, and thereafter it remains constant.[20] The constant relaxivity above 1:3 $Fe^{II}/[Gd_2bpy(DTTA)_2(H_2O)_4]^{2-}$ molar ratios proves that $\{Fe[Gd_2bpy(DTTA)_2(H_2O)_4]_3\}^{4-}$ is the only complex formed and that Fe^{II} is not oxidized to Fe^{III}. Fe^{III} would be expected to form a more stable complex with the poly(amino carboxylate) than Gd^{III}, which would lead to transmetalation, and thereby to a decrease in relaxivity (the relaxivity of the released free Gd^{3+} ion is lower than that of the metallostar). Molecular modeling also indicated that the metallostar is not sterically overcrowded, that is, the pendant poly(amino carboxylate) arms on the bipyridine moieties do not represent steric hindrance to the coordination of three bpy ligands to the Fe^{II} core. The structure of the metallostar was seen to be octahedral, with Gd–Gd distances of 14.4 ± 1.6 Å (Figure 1). This value is a simple statistical average, and the exact distance at any given time will be determined by the conformation of the methylene bridges between the bipyridine and the DTTA moieties.

All metallostar samples studied were prepared by the convergent approach, that is, by first preparing the dinuclear $[Ln_2bpy(DTTA)_2(H_2O)_4]^{2-}$ complex and subsequently adding Fe^{II} to the solution. In this way, one can ensure that all of the poly(amino carboxylate) sites are occupied by the

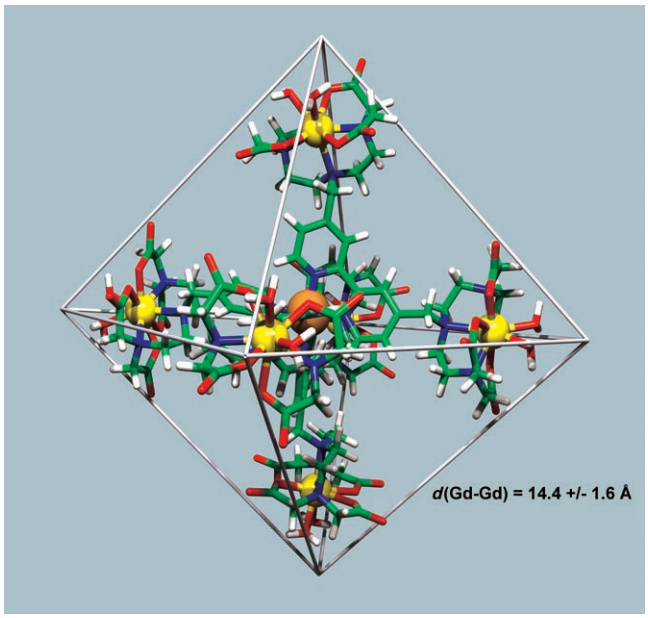

Figure 1. Molecular modeling representation of the metallostar $\{Fe[Gd_2bpy(DTTA)_2(H_2O)_4]_3\}^{4-}$.

lanthanide ions and that the iron(II) coordinates exclusively to the bpy nitrogens. When proceeding the other way around, the numerous vacant poly(amino carboxylate) sites might enter into competition with the bpy for Fe^{II} coordination, especially at higher pH, as suggested by simulations of complex stabilities for Fe^{II}–bpy–poly(amino carboxylate) systems based on literature data. Once even a small amount of Fe^{II} is coordinated to the $DTTA^{4-}$ subunit, it will shift the equilibrium by accelerating the oxidation of Fe^{II} to Fe^{III}, since the poly(amino carboxylate) forms a very stable complex with Fe^{III}. This is nicely demonstrated by comparing the ^1H NMR spectra of an $\{Fe[Y_2bpy(DTTA)_2(H_2O)_4]_3\}^{4-}$ metallostar sample prepared by the usual convergent approach with that of another sample prepared by first adding Fe^{II} to the $bpy(DTTA)_2^{8-}$ ligand and then adding an equimolar amount of Y^{III} (Figure 2). In the second case, one ob-

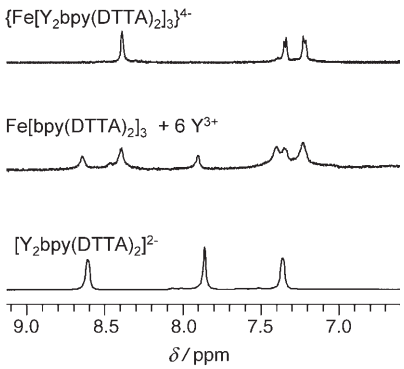

Figure 2. Signals of bipyridine protons in the ^1H NMR spectra of the metallostar $\{Fe[Y_2bpy(DTTA)_2(H_2O)_4]_3\}^{4-}$, prepared by adding a stoichiometric amount of Fe^{2+} to the dinuclear $[Y_2bpy(DTTA)_2(H_2O)_4]^{2-}$ (convergent approach) (top), $Fe[bpy(DTTA)_2]_3$ + six molar equivalents of Y^{3+} (middle), and $[Y_2bpy(DTTA)_2(H_2O)_4]^{2-}$ (bottom); pH 6.0 for all samples.

serves two sets of bpy proton signals in the spectrum, one set corresponding to the metallostar, identical to the signals observed for the sample prepared by the convergent approach, and another set attributable to the free, non-iron(II)-coordinated bpy protons, as observed for the dinuclear complex $[Y_2bpy(DTTA)_2(H_2O)_4]^{2-}$. This sample was prepared and kept in a normal NMR tube and no particular attention was paid to the exclusion of air. As a result, a considerable amount of Fe^{II} was oxidized, since the two series of bpy proton peaks indicate comparable concentrations of the free and the Fe^{II}-coordinated states. Such significant oxidation does not occur in a sample prepared by the convergent approach, even when it is fully exposed to air. Even without a detailed study, we can state that the free poly(amino carboxylate) sites contribute very strongly to the oxidation of Fe^{II} to Fe^{III}.

pH-potentiometry: The protonation constants, $\log K_{Hi}$, of $H_8bpy(DTTA)_2$, defined as in Equation (1), were determined by pH-potentiometric titration at $I = 0.1$ M $(CH_3)_4NCl$, 25 °C.

$$K_i^H = \frac{[H_iL]}{[H_{i-1}L][H^+]} \quad (1)$$

The titration curves were evaluated by assuming that the two poly(amino carboxylate) units behave independently and thus identically. The system was described as the sum of two series of protonation sites (as though there were two independent ligands in solution), one for the poly(amino carboxylate) and one for the bipyridine, present in a 2:1 concentration ratio. Four protonation constants for the poly(amino carboxylate) moiety and two for the bipyridine unit could be determined. The titration curves are presented in Figure 3 and the calculated protonation constants are shown in Table 1. In comparison to $TTAHA^{6-}$ or $DTPA^{5-}$, the first protonation constant of the poly(amino carboxylate) entity of $bpy(DTTA)_2^{8-}$ is somewhat lower. This $\log K_{H1}$ value characterizes the protonation of the central amine nitrogen, which is evidently affected by the attachment of the bipyridine unit. However, since there is a methylene linking group between the poly(amino carboxylate) and the bipyridine, the basicity decrease of this central nitrogen as compared to that in $DTPA^{5-}$ is much more limited than in the case of the tpy-$DTTA^{4-}$ ligand, in which the aromatic ring is directly attached to the amine nitrogen.[19] Consequently, one would expect a higher stability constant for the Gd^{III} complex of $[bpy(DTTA)_2]^{8-}$ than for that with tpy-$DTTA^{4-}$. By analogy with similar poly(amino carboxylate) ligands, for which ^1H NMR titrations have been performed to assess the protonation scheme,[19,23,24] the second protonation step most likely occurs on one of the terminal nitrogens and is accompanied by transfer of the first proton from the central to the other terminal nitrogen. The third proton is then shared between the central nitrogen and a carboxylate, and the subsequent $\log K_{H4}$ constant can be attributed to protonation of a carboxylate.

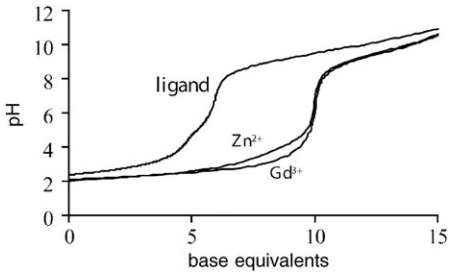

Figure 3. pH-potentiometric titration curves obtained by titrating a solution of $H_{10}bpy(DTTA)_2^{2+}$ alone (ligand) and in the presence of two equivalents of Gd^{3+} and Zn^{2+} with $(CH_3)_4NOH$; $T = 298$ K.

We also performed pH-potentiometric titrations on an Fe-$[bpy(DTTA)_2]_3^{22-}$ solution without Gd^{III}, which allowed us to determine the first two protonation constants of the poly(amino carboxylate) ligand with the bipyridine coordinated to the Fe^{II}. Based on the stability constant of the $Fe(bpy)_3$ complex reported in the literature ($\log\beta = 17.45$),[25] at the concentration used for our pH-potentiometric titration a partial dissociation of the $Fe(bpy)_3$ core occurs at pH < 3.8, which prevents determination of the lower protonation constants of the poly(amino carboxylate) unit. The two protonation constants calculated for the amine nitrogens in Fe-$[bpy(DTTA)_2]_3$ are slightly higher than those for the free ligand.

Concerning the bipyridine unit, both protonation constants calculated for $[bpy(DTTA)_2]^{8-}$ are somewhat higher

Table 1. Protonation constants of various ligands and stability constants of their complexes, determined by pH-potentiometry. $I = 0.1$ M $(CH_3)_4NCl$, 25 °C.

Ligand	$[bpy(DTTA)_2]^{8-}$	$[Fe\{bpy(DTTA)_2\}_3]^{22-}$	$(tpy\text{-}DTTA)^{4-}$[a]	$TTAHA^{6-}$[b]	$DTPA^{5-}$[c]
$\log K_{H1}$[d]	9.87(3)	10.18(3)	8.65	10.66	10.41
$\log K_{H2}$[d]	9.16(3)	9.29(2)	7.63	8.56	8.37
$\log K_{H3}$[d]	3.09(4)			8.38	4.09
$\log K_{H4}$[d]	1.5(2)			2.92	2.51
$\log K_{H1bpy}$[e]	5.51(4)		5.25[f]		
	4.4(2)[g]				
$\log K_{H2bpy}$[e]	2.1(3)		3.30[f]		
$\log K_{GdL}$	18.2(2)		10.87(1)	19.0	22.5
$\log K_{GdHL}$	–		3.73(3)	8.3	1.8
$\log K_{ZnL}$	18.0(2)		–	18.9	18.3
$\log K_{ZnHL}$	3.4(2)		–	8.0[h]	3.0
p*Gd*[i]	14.9		10.6	15.5	19.1

[a] From ref. [19]. [b] From ref. [28]. [c] From ref. [26]. [d] Protonation constants of the poly(amino carboxylate) moiety. [e] Protonation constants of the bipyridine moiety. [f] Protonation constants of terpyridine nitrogens. [g] Determined for $[Y_2bpy(DTTA)_2]^{2-}$ by ^1H NMR titration. [h] 3.68 and 2.33 for $\log K_{H2ZnL}$ and $\log K_{H3ZnL}$, respectively. [i] $-\log[Gd_{free}]$ at pH 7.4, $c_{Gd} = 1$ μM, $c_L = 10$ μM.

than the literature values for the unsubstituted bipyridine (5.51 and 2.1 versus 4.4 and 1.5; $I = 0.1$ M; 25 °C).[26] We also wanted to assess the bipyridine protonation constant in the dinuclear Ln^{III} complex. This was probed by a ^1H NMR titration of the diamagnetic chelate $[Y_2bpy(DTTA)_2(H_2O)_4]^{2-}$ (Figure 4). The signals of the bipyridine unit are well separated from those of the poly(amino carboxylate) protons and could be easily used to calculate the first protonation constant, $\log K_{Hbpy1} = 4.4(1)$, which is 1 log unit lower than that in the free $bpy(DTTA)_2^{8-}$ ligand and corresponds exactly to the value published for the bpy core without $DTTA^{4-}$ subunits. The determination of the second protonation constant was not possible due to decomposition of the complex at lower pH.

Complex stability constants, $\log K_{ML}$, and complex protonation constants, $\log K_{MHL}$ [Eqs. (2) and (3)], have been determined for the dinuclear complexes formed with Gd^{III} and Zn^{II} by direct potentiometric titrations. Here again, we considered the two poly(amino carboxylate) units to be identical, and accordingly, in Equation (2) L defines the equilibrium concentration of the uncomplexed diethylenetriaminetetraacetate moiety.

$$K_{ML} = \frac{[ML]}{[M][L]} \quad (2)$$

$$K_{MHL} = \frac{[MHL]}{[H][ML]} \quad (3)$$

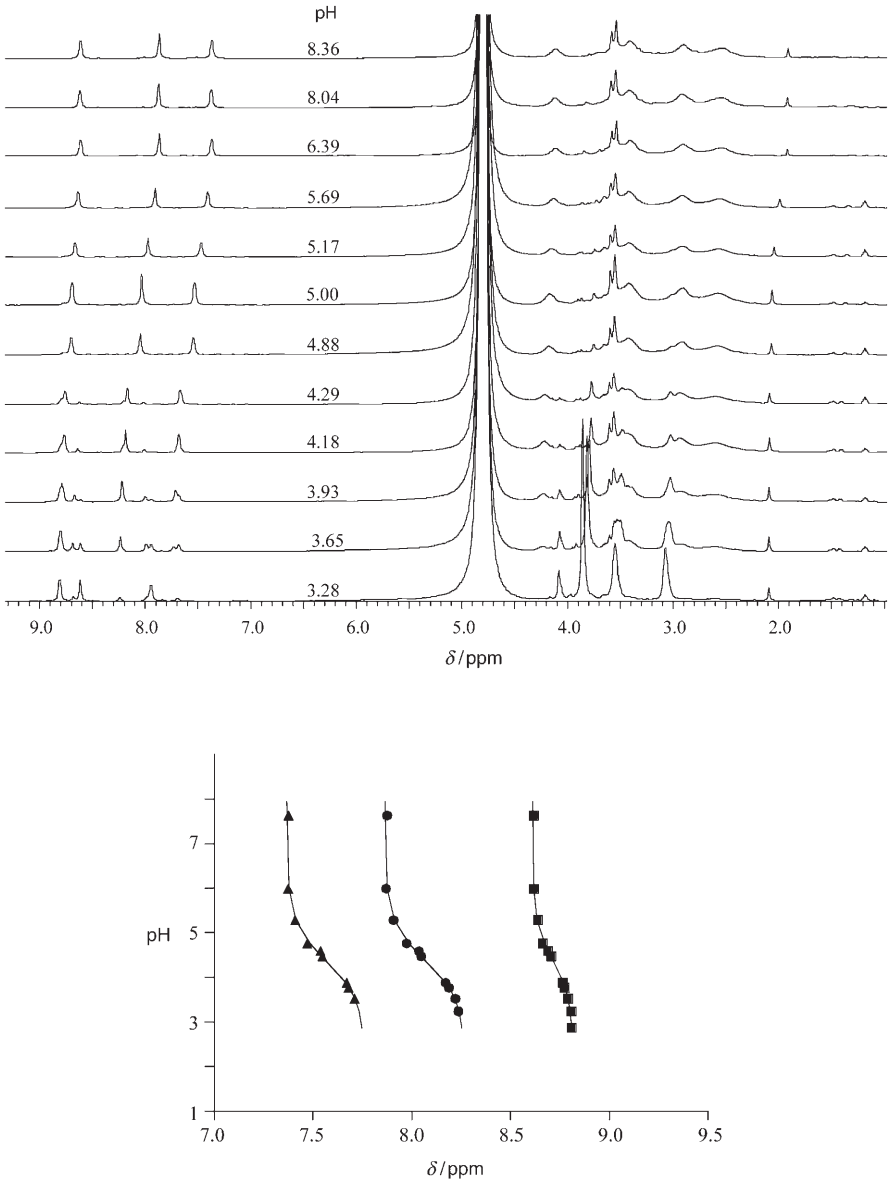

Figure 4. Variable-pH ^1H NMR spectra of $[Y_2bpy(DTTA)_2(H_2O)_4]^{2-}$ (top) and the titration curves obtained for the protons of the bipyridine moiety (bottom).

Due to decomposition of the $Fe(bpy)_3$ core under the acidic conditions required for the formation of the Gd^{III} or Zn^{II} complexes with the poly(amino carboxylate) part, it was not possible to determine Gd^{III} and Zn^{II} stability constants for the metallostar. However, we consider that the coordination of the bpy moiety to the Fe^{II} does not significantly modify the stability constant of the poly(amino carboxylate) complexes.

Zn^{2+} is one of the most abundant endogenous metal ions, and it is usually accepted that the in vivo safety of a GdL complex can be directly related to the selectivity of the ligand for Gd^{III} versus Zn^{II}, expressed as the ratio of the two thermodynamic stability constants.[27] The stability constant of the Gd^{III} complex of our ligand is remarkably higher than that with tpy-$DTTA^{4-}$,[19] which can be mainly ascribed to the different basicities of the central nitrogens. The $\log\beta$ value is comparable to that reported for $[Gd(TTAHA)(H_2O)_2]^{3-}$,[28] as expected on the basis of their identical, heptadentate chelating units, while it is 4 log units lower than the stability constant of the Gd complex formed with the octadentate $DTPA^{5-}$.[26] The p*Gd* value calculated under the commonly used conditions (pH 7.4, $c_{Gd} = 1\,\mu M$, $c_L = 10\,\mu M$)[29] is 14.9, which greatly

exceeds the p*Gd* of 10.6 for $\{Fe^{II}[Gd(tpy\text{-}DTTA)(H_2O)_2]_2\}$, but is nevertheless still lower than those of marketed MRI contrast agents (Table 1).

^{1}H NMR studies in solution: To gain some insight into the solution structure of the dinuclear complexes, we carried out a variable-temperature ^{1}H NMR study on the Eu^{III} analogue, $[Eu_2bpy(DTTA)_2(H_2O)_4]^{2-}$ (Figure 5). For the $DTTA^{4-}$ chelating unit coordinated to the paramagnetic lanthanide ion, one expects 16 peaks, which are indeed well-separated in the low-temperature spectrum. The signals due to the bpy moiety that is not directly linked to the Eu^{III} do not experience the strong paramagnetic effect and thus are not shifted from the diamagnetic region. With increasing temperature, an exchange process takes place resulting in a broadening and then coalescence of the signals. Very similar temperature dependence of the ^{1}H NMR spectra has been observed for $\{M^{II}[Eu(tpy\text{-}DTTA)(H_2O)_2]_2\}$ ($M = Fe^{II}$, Ru^{II})[19] and *m,p*-$X[(EuDTTA)(H_2O)_2]_2^{2-}$,[30] which indicates that this dynamic behavior is characteristic of the Ln-$(DTTA)^-$ subunit and is not significantly influenced by the rest of the molecule.

^{17}O NMR and ^{1}H NMRD measurements: In a preliminary communication, we reported a remarkably high relaxivity for the dinuclear $[Gd_2bpy(DTTA)_2(H_2O)_4]^{2-}$ itself, as compared to previously studied dinuclear complexes such as $pip[GdDO3A(H_2O)]_2$ and $bisoxa[GdDO3A(H_2O)]_2$ (12.5 $mM^{-1}s^{-1}$ *vs.* 5.58 and 4.43 $mM^{-1}s^{-1}$, respectively; 40 MHz, 37 °C; Scheme 2).[31] This difference was qualitatively attributed to the two inner-sphere water molecules and their faster exchange, as well as to the limited internal flexibility of $[Gd_2bpy(DTTA)_2(H_2O)_4]^{2-}$. The formation of the large and rigid $\{Fe[Gd_2bpy(DTTA)_2(H_2O)_4]_3\}^{4-}$ metallostar from $[Gd_2bpy(DTTA)_2(H_2O)_4]^{2-}$ further increases the rotational correlation time, τ_R, which results in a substantial relaxivity gain. Now, with the objective of determining the water-exchange rate and quantitatively assessing the rotational dynamics of the dinuclear $[Gd_2bpy(DTTA)_2(H_2O)_4]^{2-}$ complex and the $\{Fe[Gd_2bpy(DTTA)_2(H_2O)_4]_3\}^{4-}$ metallostar, we have performed a variable-temperature, multiple field ^{17}O NMR study on both compounds. ^{17}O longitudinal and transverse relaxation rates and chemical shifts have been measured in aqueous solutions of $[Gd_2bpy(DTTA)_2(H_2O)_4]^{2-}$ and $\{Fe[Gd_2bpy(DTTA)_2(H_2O)_4]_3\}^{4-}$ at 4.7 and 9.4 T. Additionally, ^{1}H NMRD profiles have been recorded at proton Larmor frequencies in the range 0.01–600 MHz at three different temperatures (5 °C, 25 °C, and 37 °C).

For both systems, the ^{17}O reduced transverse relaxation rates ($1/T_{2r}$) increase at the lowest temperatures, while above 285 K they decrease with temperature (slow- and fast-exchange regions, respectively; Figure 6 and Figure 7). In the slow-exchange regime, it is exclusively the water-exchange rate that determines $1/T_{2r}$. In the fast-exchange region, the reduced transverse relaxation rate is defined by the transverse relaxation rate of the bound water oxygen, $1/T_{2m}$, influenced by k_{ex}, the longitudinal electronic relaxation rate, $1/T_{1e}$, and the scalar coupling constant, $A/\hbar$. The reduced ^{17}O chemical shifts are determined by $A/\hbar$ and, to a small extent, by an outer-sphere contribution characterized by a constant, C_{OS}. Transverse ^{17}O relaxation is governed by the scalar relaxation mechanism, and thus contains no information on the rotational motion of the system. In contrast to $1/T_{2r}$, the longitudinal ^{17}O relaxation rates, $1/T_{1r}$, are determined by dipole-dipole and quadrupolar relaxation mechanisms, both related to rotation. The dipolar term depends on the gadolinium(III)–water oxygen distance, r_{GdO}, while the quadrupolar term is influenced by the quadrupolar coupling constant, $\chi(1+\eta^2/3)^{1/2}$. Proton relaxivities are influenced by a large number of factors, the most important being water exchange, rotation, and electron spin relaxation.

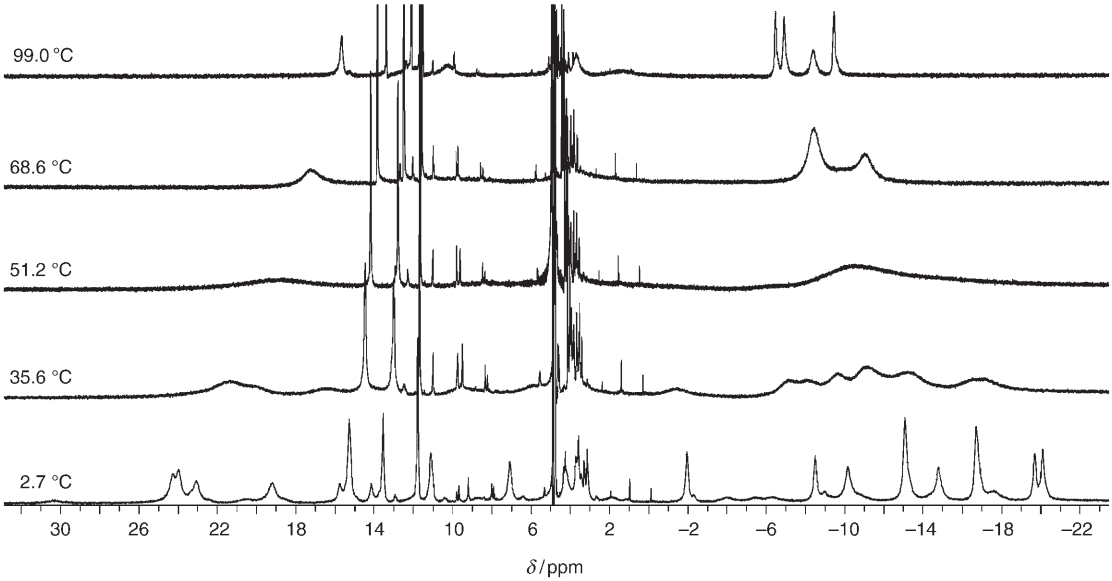

Figure 5. Variable-temperature, 400 MHz ^{1}H NMR spectra of $[Eu_2bpy(DTTA)_2(H_2O)_4]^{2-}$; pH 6.2.

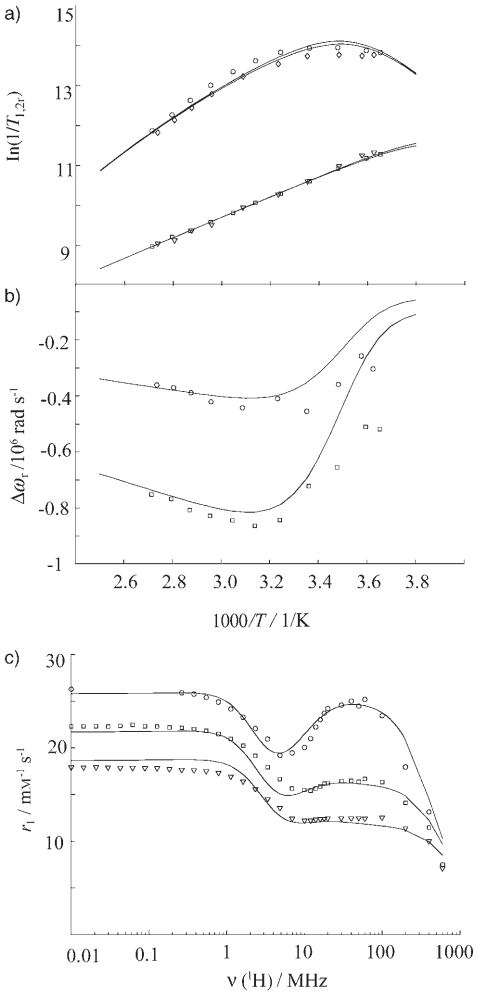

Figure 6. $[Gd_2bpy(DTTA)_2(H_2O)_4]^{2-}$: Temperature dependence of a) reduced transverse $1/T_{2r}$ (9.4 T (○) and 4.7 T (◇)) and longitudinal ^{17}O relaxation rates $1/T_{1r}$ (9.4 T (□) and 4.7 T (▽)); b) reduced chemical shifts $\Delta\omega_r$ (9.4 T (□) and 4.7 T (○)); c) ^1H nuclear magnetic relaxation dispersion profiles, recorded at 5 °C (○), 25 °C (□), and 37 °C (▽). The lines represent the least-squares simultaneous fitting of all data points, as explained in the text.

For $[Gd_2bpy(DTTA)_2(H_2O)_4]^{2-}$, the experimental ^{17}O NMR and ^1H NMRD data were analyzed simultaneously (for the equations used, see the Supporting Information) and are shown together with the fitted curves in Figure 6. For $\{Fe[Gd_2bpy(DTTA)_2(H_2O)_4]_3\}^{4-}$ (Figure 7), a simultaneous analysis of ^{17}O and ^1H relaxation data was not possible; in particular, an acceptable fit of the ^{17}O transverse relaxation rates seemed to be incompatible with the low-field NMRD data. Such a discrepancy most probably originates from an inadequate description of the electron spin relaxation. Indeed, electron spin relaxation has a strong influence on both the low-field proton relaxivities and the transverse ^{17}O relaxation rates in the intermediate and fast water-exchange regimes. The magnetic field difference is relatively significant between the low frequency part of the NMRD curve (<0.02 T) and the ^{17}O data (4.7 and 9.4 T). Without an appropriate theory that is capable of describing the field dependence of electron spin relaxation rates over such a large range, it is impossible to perform a simultaneous fitting of the ^1H and ^{17}O relaxation data. Significant progress in the theoretical understanding of electron spin relaxation of Gd^{III} complexes has recently been achieved with the inclusion of both transient and static zero-field splitting (ZFS).[32] However, this new theory only applies to small molecules and fails in the case of medium-sized complexes, such as our metallostar. Therefore, we were obliged to apply the theory of electron spin relaxation as described by the traditional Solomon–Bloembergen–Morgan equations. Powell's approach[31] was used, where $1/T_{ie}$ is the sum of a transient ZFS and a so-called spin-rotation (SR) contribution. The ZFS term is described by the trace of the squared ZFS tensor, Δ^2, a correlation time τ_v, and an activation energy E_v (fixed at 1 kJ mol^{-1}); the SR term is characterized by a δg_L^2 parameter. For the fitting, we proceeded in the following way: the transverse ^{17}O relaxation rates, which give access first of all to the water-exchange rate, were fitted together with the ^{17}O chemical shifts. The scalar coupling constant, the rate, activation enthalpy, and entropy of the water exchange were obtained from this fitting, as well as the parameters of the electron spin relaxation. In a second step, we fitted together the longitudinal ^{17}O relaxation rates and the ^1H relaxivities, both containing primary information on the rotational dynamics. Here, we fixed the water-exchange parameters at the values obtained from the previous fitting of ^{17}O $1/T_{2r}$ and $\Delta\omega_r$ data, and calculated rotational and electronic parameters, the latter being almost exclusively determined by proton relaxivities and not by ^{17}O longitudinal relaxation. It should be noted that including the ^{17}O longitudinal relaxation rates in the fitting of the transverse rates and chemical shifts does not influence the parameters obtained for the water exchange or the scalar coupling constant. The advantage of separately fitting ^{17}O $1/T_{2r}$ with $\Delta\omega_r$ and ^{17}O $1/T_{1r}$ with proton relaxivities is that the first data series defines water exchange while the second defines rotation with high accuracy. As expected, the electronic parameters obtained from the two fittings are different: $\tau_v^{298} = 15\pm5$ ps, $\Delta^2 = (0.66\pm0.20)\times10^{20}$ s^{-2}, and $\delta g^2_L = 0.10\pm0.02$ from the analysis of ^{17}O $1/T_{2r}$ and $\Delta\omega_r$ values; $\tau_v^{298} = 27\pm8$ ps, $\Delta^2 = (0.18\pm0.05)\times10^{20}$ s^{-2}, and $\delta g^2_L = 0.01\pm0.02$ from the analysis of NMRD and ^{17}O $1/T_{1r}$. We are aware of the shortcomings of the electron spin relaxation theory used, and thus interpretation of these values in terms of physical meaning is not possible. For the dinuclear $[Gd_2bpy(DTTA)_2(H_2O)_4]^{2-}$ we obtained $\tau_v^{298} = 34\pm2$ ps, $\Delta^2 = (0.17\pm0.01)\times10^{20}$ s^{-2}, and $\delta g^2_L = 0.10\pm0.06$ by a simultaneous fitting of ^{17}O and ^1H relaxation data.

In the fitting procedure, r_{GdO} was fixed at 2.50 Å, based on available crystal structures[33,34] and recent ESEEM results.[35] The Gd^{III}–H distance, r_{GdH}, was set at 3.10 Å,[36] the distance of closest approach of an outer-sphere water proton to the gadolinium(III), a_{GdH}, was set at 3.5 Å,[30] and for the quadrupolar coupling constant, $\chi(1+\eta^2/3)^{1/2}$, we used the value for pure water, 7.58 MHz. The C_{os} empirical constant, characterizing the outer-sphere contribution to the ^{17}O

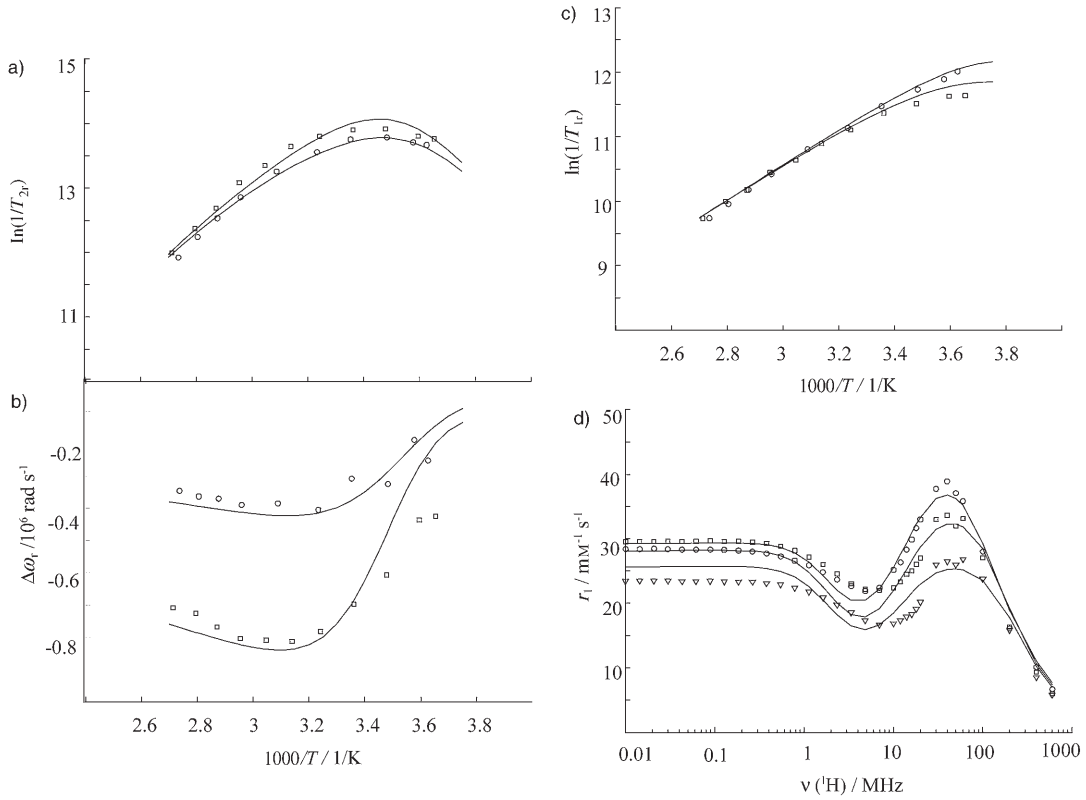

Figure 7. $\{Fe[Gd_2bpy(DTTA)_2(H_2O)_4]_3\}^{4-}$: Temperature dependence of a) reduced transverse $1/T_{2r}$ ^{17}O relaxation rates (9.4 T (□) and 4.7 T (○)), b) reduced chemical shifts $\Delta\omega_r$ (9.4 T (□) and 4.7 T (○)); c) longitudinal $1/T_{1r}$ ^{17}O relaxation rates (9.4 T (□) and 4.7 T (○)); d) ^1H nuclear magnetic relaxation dispersion profiles, recorded at 5 °C (○), 25 °C (□), and 37 °C (▽). The lines represent the least-squares simultaneous fitting of data points of (a) with (b) and of (c) with (d), as explained in the text.

chemical shifts, was fixed at 0.1. The diffusion constant, D_{GdH}^{298}, used in the analysis of ^1H NMRD data, and the corresponding activation energy, E_{GdH}, were fitted to $D_{GdH}^{298} = (24.1 \pm 2.0) \times 10^{-10}\,m^2\,s^{-1}$ and $(20.0 \pm 1.0) \times 10^{-10}\,m^2\,s^{-1}$ and $E_{GdH} = 33 \pm 4$ and $23 \pm 4\,kJ\,mol^{-1}$ for $[Gd_2bpy(DTTA)_2(H_2O)_4]^{2-}$ and $\{Fe[Gd_2bpy(DTTA)_2(H_2O)_4]_3\}^{4-}$, respectively.

The ^{17}O longitudinal relaxation rates measured for $\{Fe[Gd_2bpy(DTTA)_2(H_2O)_4]_3\}^{4-}$ were different at 4.7 and 9.4 T, which is always indicative of slow rotational motion. In such cases, the ^{17}O and ^1H relaxation rates can be conveniently analyzed by means of the Lipari–Szabo model-free approach,[16] which has been previously applied for the evaluation of NMR relaxation data for various macromolecular systems. This approach allows the separation of two kinds of motions that modulate relaxation: a rapid local motion characterized by a correlation time τ_l (activation energy E_l) and a slow global motion with a correlation time τ_g (activation energy E_g). The global rotational times, τ_g, obtained from either ^{17}O NMR or ^1H NMRD, represent the same overall motion of the system ($\tau_{gO} = \tau_{gH}$), while the local rotational correlation times, τ_{lO} and τ_{lH}, might be different as they are attributed to the motion of the $Gd–O_{water}$ and $Gd–H_{water}$ vectors, respectively. The ratio of the two rotational correlation times τ_{lH}/τ_{lO} was generally found to be ~0.65 for monohydrated complexes,[37,38] while for bishydrated chelates, values close to 1 were obtained from the simultaneous fitting of longitudinal ^{17}O and ^1H relaxation rates.[19,39] Finally, a model-independent measure of the spatial restriction of the local motion is given by the generalized order parameter, S^2. For an isotropic internal motion $S^2 = 0$, while for a fully restricted motion $S^2 = 1$.

All parameters obtained by this fitting are reported in Table 2 and Table 3.

Water exchange: The diethylenetriamine-tetraacetate unit that coordinates the Gd^{III} ion has seven donor atoms (three amine nitrogens and four carboxylate oxygens). Assuming a coordination number of nine for the lanthanide ion, which is the most common in similar poly(amino carboxylate) complexes, two water molecules complete the inner coordination sphere in aqueous solution. Unfortunately, all efforts to obtain appropriate crystals for X-ray analysis of either the dinuclear $[Gd_2bpy(DTTA)_2(H_2O)_4]^{2-}$ or the metallostar met with failure. The solid-state X-ray crystal structure reported for $[C(NH_2)_3]_3[Gd(TTAHA)]\cdot 9H_2O$ was also indicative of an N_3O_4 donor set provided by the ligand, which was completed by the coordination of two carboxylate oxygens from a neighboring complex.[40] In aqueous solution, these two carboxylates are replaced by water molecules, as was proven by the ^{17}O NMR chemical shifts.[22]

Table 2. Water-exchange parameters determined for various $Gd^{III}L$ complexes.

Complex	q	k_{ex}^{298} [$10^6\ s^{-1}$]	$\Delta H^{\neq}$ [$kJ\,mol^{-1}$]	$\Delta S^{\neq}$ [$J\,mol^{-1}\,K^{-1}$]	$A/\hbar$ [$10^6\ rad\,s^{-1}$]	
$[Gd_2bpy(DTTA)_2(H_2O)_4]^{2-}$	2	8.1 ± 0.3	43.7 ± 2.1	$+34\pm6$	-3.7 ± 0.3	this work
$\{Fe[Gd_2bpy(DTTA)_2(H_2O)_4]_3\}^{4-}$	2	7.4 ± 0.2	41.3 ± 3.0	$+25\pm8$	-3.9 ± 0.2	this work
$[Gd(HTTAHA)(H_2O)_2]^-$	2	8.6	40.4	+23.3	−3.5	[22]
$\{Fe^{II}[Gd(tpy\text{-}DTTA)(H_2O)_2]_2\}$	2	5.1	39.6	+16.4	−3.7	[19]
m-$X[Gd(DTTA)(H_2O)_2]_2^{2-}$	2	8.9	39.2	+23.6	−3.4	[39]
$[Gd(DTPA)(H_2O)]^{2-}$	1	3.3	51.6	+53.0	−3.8	[31]

Table 3. Rotational parameters determined for various $Gd^{III}L$ complexes.

Complex	τ_{gO}^{298} [ps]	τ_{lO}^{298} [ps]	S^2
$[Gd_2bpy(DTTA)_2(H_2O)_4]^{2-}$	240 ± 10[a]		
$\{Fe^{II}[Gd(tpy\text{-}DTTA)(H_2O)_2]_2\}$	410[a]		
$\{Fe[Gd_2bpy(DTTA)_2(H_2O)_4]_3\}^{4-}$	930 ± 50	190 ± 15	0.60 ± 0.04
dendrimers			
Gadomer 17[b]	3050	760	0.50
G5-(GdEPTPA)111 (pH 6.0)[c]	4040	150	0.43
micelles			
[Gd(DOTAC12)][d]	1600	430	0.23
[Gd(DOTAC14)][d]	2220	820	0.17
[Gd(DOTASAC18)][d]	2810	330	0.28

[a] No Lipari–Szabo treatment; a single τ_R^{298} is calculated; for $\{Fe^{II}[Gd(tpy\text{-}DTTA)(H_2O)_2]_2\}$; ref. [19]. [b] From ref. [10]. [c] From ref. [11]. [d] From ref. [12].

The assessment of the hydration state of a Gd^{III} complex in solution is often considered to be problematic. Luminescence lifetime measurements on the Eu^{III} and Tb^{III} analogues are commonly used to determine the hydration number, q.[41] The lanthanide-induced ^{17}O shifts are directly related to the number of water molecules in the inner coordination sphere and can therefore be straightforwardly used to assess q. This method is generally applied for Dy^{III} complexes,[42] but it is also applicable for Gd^{III} chelates. The ^{17}O chemical shifts measured at the two magnetic fields for both $[Gd_2bpy(DTTA)_2(H_2O)_4]^{2-}$ and $\{Fe[Gd_2bpy(DTTA)_2(H_2O)_4]_3\}^{4-}$ correspond to bishydrated complexes. Indeed, the scalar coupling constants calculated with $q = 2$ are typical for a Gd^{III} poly(amino carboxylate).

For the water-exchange rate, we obtained $k_{ex}^{298} = 8.1\times10^6$ and $7.4\times10^6\ s^{-1}$ for $[Gd_2bpy(DTTA)_2(H_2O)_4]^{2-}$ and $\{Fe[Gd_2bpy(DTTA)_2(H_2O)_4]_3\}^{4-}$, respectively. These values, as well as the activation enthalpies and entropies, compare well with those reported for Gd^{III} chelates containing an identical diethylenetriamine-tetraacetate chelating unit, such as the parent $[Gd(TTAHA)(H_2O)_2]^{3-}$, the dinuclear *p*,*m*-$X[GdDTTA(H_2O)_2]_2$, and $\{Fe^{II}[Gd(tpy\text{-}DTTA)(H_2O)_2]_2\}$ (Table 2). The faster water exchange of these chelates as compared to that in the diethylenetriamine-pentaacetate $[Gd(DTPA)(H_2O)]^{2-}$ can be related to the presence of the two inner-sphere water molecules. These contribute to an increased flexibility of the inner sphere, which can then rearrange more easily in the course of the water-exchange process. However, the water-exchange rate is slightly lower than the optimal value required by the Solomon–Bloembergen–Morgan theory to attain maximum proton relaxivities ($\sim50\times10^6\ s^{-1}$). The values of the activation entropy and enthalpy point to a dissociatively activated exchange, as indeed is to be expected for a nine-coordinate complex. A variable-pressure ^{17}O NMR study performed on the complex $\{Fe^{II}[Gd(tpy\text{-}DTTA)(H_2O)_2]_2\}$, having the same $DTTA^{4-}$ Gd^{III}-chelating part, resulted in an activation volume of $\Delta V^{\neq} = +6.8\ cm^3\,mol^{-1}$, thus providing experimental evidence for a dissociatively activated interchange water-exchange mechanism.[19]

Rotational dynamics: The rotational motion of the dinuclear complex could be adequately described by a single correlation time (Table 3); the molecule is too small to distinguish between global and local motions. The value of τ_{RO}^{298} corresponds well with the size of the molecule and is in accordance with previously measured values for similar sized chelates. For the metallostar, the local motion of the Gd-coordinated water proton vector could be separated from the overall motion of the molecule, and was found to be about five times faster than the tumbling of the entire metallostar. The global rotational correlation time is less than 1 ns, which is considerably smaller than values reported for macromolecular systems such as dendrimers, linear polymers, or micellar aggregates. The difference between τ_{lO}^{298} and τ_{gO}^{298} unambiguously proves that the metallostar is not completely rigid. However, based on the relatively high value of the S^2 parameter, which describes the restriction of the local motions with respect to the global one, its flexibility is limited in comparison with macromolecules previously analyzed by the Lipari–Szabo approach. Indeed, the value of S^2 is considerably higher than those for micellar systems, and also exceeds S^2 values calculated for dendrimers (Table 3). In the metallostar, the $Fe(bpy)_3$ core can be considered to be completely rigid. This also applies for extended, metallodendrimeric edifices, which is a clear advantage of such self-assembled systems. The only point of flexibility in the metallostar is the methylene group that connects the bipyridine moiety to the poly(amino carboxylate) part, which was introduced in order to maintain sufficient thermodynamic stability (vide infra). Indeed, no field dependence of the longitudinal ^{17}O relaxation rates, and thus no internal flexibility, was detected for $\{Fe^{II}[Gd(tpy\text{-}DTTA)(H_2O)_2]_2\}$, in which the poly(amino carboxylate) part is directly linked to the terpyridine unit.[19]

Proton relaxivity: Owing to its larger size and slower tumbling, the relaxivities are considerably higher for the metallostar than for the dinuclear complex at almost all frequencies, with a maximum difference at 30–60 MHz. However, the temperature dependence at the maximum of the relaxivity peak indicates that the relaxivity is still limited by rotation. Remarkably, the metallostar has an unusually broad high-field relaxivity peak centered at relatively high fre-

quencies. This originates from its moderate size and the consequent rotational correlation time. This feature is particularly important since higher and higher fields (>60 MHz) are being utilized in clinics to increase sensitivity, and at such high magnetic fields the large macromolecular contrast agents, such as dendrimers, offer barely better performances than the marketed small chelates. Indeed, the Solomon–Bloembergen–Morgan theory predicts that at frequencies above about 200 MHz the relaxivity should increase with the inverse of the rotational correlation time, while at lower frequencies it should be proportional to τ_R. This implies that at high fields intermediate-sized molecules are favorable compared to very large ones. This theoretically predicted effect is nicely reflected in the high-field descending part of the relaxivity profiles measured for the metallostar at variable temperature. At 200 MHz, there is an inversion of the temperature dependence of the experimental data: at lower frequencies, the relaxivity increases with decreasing temperature since the rotation becomes slower, while at higher frequencies, this tendency is reversed. To the best of our knowledge, this is the first experimental observation of this phenomenon.

In the context of MRI contrast agents, the molar relaxivity calculated per Gd is most widely used as a measure of efficacy. For certain applications, however, it is not the most appropriate parameter. In targeting approaches, a large paramagnetic effect has to be delivered into a restricted space, that is, the contrast agent molecule not only has to bear efficient Gd^{III} sites (high molar relaxivity), but they also have to be "densely" located. In this respect, a large macromolecule with few Gd^{III} centers of even very high molar relaxivity might be less favorable than a medium-sized molecule with densely packed Gd^{III} ions. In order to express this feature, we have recently introduced the concept of mass relaxivity or density of relaxivity,[20] which defines the relaxation rate enhancement in terms of unit mass of the agent, as given in Equation (4), where n_{Gd} is the number of Gd centers per molecule, and M_w is the molecular mass of the complex (the multiplication factor of 1000 is to obtain convenient numbers).

$$\text{"}\textit{density of relaxivity}\text{"} = \frac{r_1 \times n_{Gd}}{M_w} \times 1000 \quad \left(\frac{\text{mM}^{-1}\,\text{s}^{-1}}{\text{gmol}^{-1}} \text{ or } (\text{g/L})^{-1}\,\text{s}^{-1}\right) \tag{4}$$

The molar relaxivity of the metallostar is very high, comparable with that of high generation dendrimers (27.0 and 33.2 $\text{mM}^{-1}\text{s}^{-1}$ at 25 °C for $\{Fe[Gd_2bpy(DTTA)_2(H_2O)_4]_3\}^{4-}$ versus 36 and 27 $\text{mM}^{-1}\text{s}^{-1}$ at 23 °C for a tenth generation GdDOTA-loaded dendrimer at 20 and 60 MHz, respectively).[43] With six Gd^{III} ions incorporated in a relatively low molecular mass of 3744 g mol^{-1}, the metallostar represents a highly powerful contrast agent in terms of efficacy per unit mass. Indeed, this compound offers the most concentrated paramagnetic relaxation effect among all Gd^{III}-based potential contrast agents reported to date (Table 4).

Stability tests on the metallostar: Biological fluids are very complex systems, in which the injected contrast agent may be exposed to diverse chemical interactions. For a typical Gd^{III} complex, transmetalation reactions with Cu^{II} and Zn^{II} are usually considered as the most significant steps leading to decomposition of the complex. The free Gd^{III} released in this way can, in turn, react with endogenously available small chelators, such as citrate, phosphate, etc. In the case of the metallostar, an additional instability factor stems from the iron(II)–bipyridine coordination. In order to obtain some information on the stability of the metallostar under biologically relevant conditions, we monitored proton relaxivity over a long period of time in phosphate-buffered saline (PBS) as well as in mouse serum. The samples were prepared with degassed water and were kept under nitrogen. As shown in Figure 8, in mouse serum and PBS the relaxivity decreases sharply with time; although the time course of the decomposition process is relatively long, the decays could be fitted by mono-exponential functions that gave $t_{1/2}$ values of 3.7 ± 0.3 and 4.7 ± 0.4 h in mouse serum and PBS, respectively. The relaxivity decay was reproducible in independent samples. In both cases, the relaxivity curve reaches a plateau. In mouse serum, the equilibrium value is equal to the relaxivity of the dinuclear $[Gd_2bpy(DTTA)_2(H_2O)_4]^{2-}$ chelate, showing that the $Fe(bpy)_3$ com-

Table 4. Molar proton relaxivities, r_1, and densities of relaxivity for a selection of Gd^{III} complexes; 37 °C, 20 MHz.

Type	Complex[a]	No. of Gd	M_w	r_1 [$\text{mM}^{-1}\text{s}^{-1}$]	density of relaxivity
metallostar	$\{Fe[Gd_2bpy(DTTA)_2(H_2O)_4]_3\}^{4-}$	6	3744	20.17	32.3
monomers	$[Gd(DTPA)(H_2O)]^{2-}$[b]	1	563	4.02	7.1
	$[Gd(EOB\text{-}DTPA)(H_2O)]^{2-}$[c]	1	696	5.3	7.6
	[Gd(DTPA-BMA)(H_2O)][b]	1	587	3.96	6.7
	$[Gd(HTTAHA)(H_2O)_2]^{2-}$[d]	1	683	7.3	10.7
	$[Gd(DOTA)(H_2O)]^{-}$[b]	1	575	3.83	6.7
dinuclear	$[Gd_2bpy(DTTA)_2(H_2O)_4]^{2-}$	2	1229	12.44	20.2
	$pip[Gd(DO3A)(H_2O)]_2$[b]	2	1202	5.79	9.6
	$p\text{-}X[(GdDTTA)(H_2O)_2]_2^{2-}$[e]	2	1087	12.8	23.6
	$\{Fe^{II}[Gd(tpy\text{-}DTTA)(H_2O)_2]_2\}$[f]	2	1568	15.7	20.0
dendrimers	$G3\text{-}(GdDO3A)_{23}$[g]	23	22100	14.6	15.2
	$G4\text{-}(GdDO3A)_{30}$[g]	30	37400	15.9	12.8
	$G5\text{-}(GdDO3A)_{52}$[g]	52	61800	18.7	15.7
	$G5\text{-}(GdEPTPA)_{111}$[h]	111	112055	17.1	17.5
	$G7\text{-}(GdEPTPA)_{253}$[h]	253	302680	25.6	20.3
	$G9\text{-}(GdEPTPA)_{1157}$[h]	1157	1388400	24.2	20.7

[a] EOB-$DTPA^{5-}$: ethoxybenzyl-DTPA; DTPA-BMA^{3-}: DTPA-bis(methylamide); $DOTA^{4-}$: 1,4,7,10-tetraazacyclododecane-1,4,7,10-tetraacetate; $EPTPA^{5-}$: ethylenepropylenediamine-*N*,*N*,*N*′,*N*″,*N*″-pentaacetate. [b] From ref. [31]. [c] From ref. [52]. [d] From ref. [22]. [e] From ref. [39]. [f] From ref. [19]. [g] From ref. [53]. [h] From ref. [11].

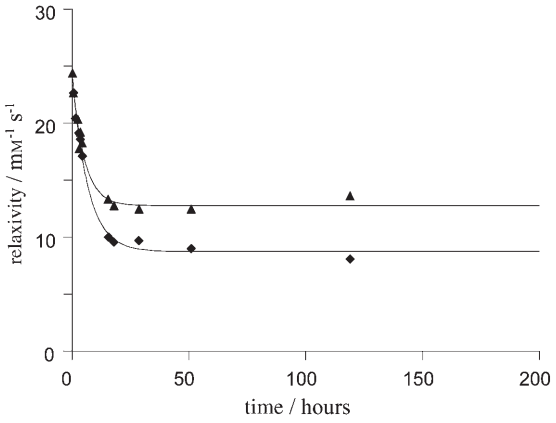

Figure 8. Decay of proton relaxivity with time for $\{Fe[Gd_2bpy(DTTA)_2(H_2O)_4]_3\}^{4-}$ in mouse serum (▲) and phosphate-buffered saline (◆). The lines represent fits of mono-exponential functions to the data points.

plex does not have sufficient long-term stability in biological media. In PBS, the equilibrium relaxivity is inferior to that of $[Gd_2bpy(DTTA)_2(H_2O)_4]^{2-}$, which points to a partial replacement of the inner-sphere water molecules by phosphate ions. The formation of ternary complexes with phosphate has been detected previously for various Gd^{III} poly(amino carboxylate) complexes.[44] Phosphate is a relatively strongly coordinating ligand towards lanthanides, and bishydrated chelates are particularly prone to ternary complex formation. It has to be noted, however, that the plasma concentration of phosphate ions is considerably lower (0.38 mM)[45] than the concentration used in the PBS buffer. As the experiment in mouse serum proves, phosphate coordination does not interfere under these conditions.

To circumvent the problem of $Fe^{II}(bpy)_3$ decomposition in biological media, Fe^{II} can be replaced by Ru^{II}, which has an extreme kinetic inertness. Previous studies on $\{Fe^{II}[Gd(tpy\text{-}DTTA)(H_2O)_2]_2\}$ and $\{Ru^{II}[Gd(tpy\text{-}DTTA)(H_2O)_2]_2\}$ showed that the two compounds behave identically with regard to their relaxation properties.[19] Ru^{II} complexes are not unknown in medical applications as they are being tested as anticancer agents. In addition, given the photophysical properties of Ru^{II}, such heterometallic Ru^{II}–Gd^{III} structures could be applied as bifunctional fluorescent and paramagnetic contrast agents. Multimodal imaging probes are indeed a focus of biomedical research since they allow for the combination of various diagnostic techniques resulting in an improved definition of diseased tissues.

Conclusion

The heterotritopic ligand $[bpy(DTTA)_2]^{8-}$ has been designed to specifically complex two Gd^{III} ions through its poly(amino carboxylate) moieties and one Fe^{II} or Ru^{II} through the bipyridine functions. We have reported herein the physicochemical characterization of the dinuclear complex $[Gd_2bpy(DTTA)_2(H_2O)_4]^{2-}$ and the metallostar $\{Fe[Gd_2bpy(DTTA)_2(H_2O)_4]_3\}^{4-}$ that forms by self-assembly when $[Gd_2bpy(DTTA)_2(H_2O)_4]^{2-}$ is treated with Fe^{II} ions. The exchange rates of the two inner-sphere water molecules are very similar in the dinuclear $[Gd_2bpy(DTTA)_2(H_2O)_4]^{2-}$ and in the metallostar and are comparable to k_{ex} for similar Gd^{III} poly(amino carboxylates) such as $[Gd(HTTAHA)(H_2O)_2]^-$ and $\{Fe^{II}[Gd(tpy\text{-}DTTA)(H_2O)_2]_2\}$. The rotational dynamics of the metallostar has been analyzed in terms of global and local motions by applying the Lipari–Szabo approach to describe the spectral density functions. This analysis was indicative of limited internal flexibility, most likely originating from the methylene group that links the Fe^{II}- and Gd^{III}-coordinating parts of the ligand. Despite this residual flexibility, the metallostar has a remarkable molar proton relaxivity, related to the two inner-sphere water molecules and their near-optimal exchange rate. Given its moderate size, the metallostar would be a particularly efficient contrast agent at very high magnetic fields (>100 MHz). The presence of six efficiently relaxing Gd^{III} ions in one metallostar leads to an exceptionally high relaxivity confined within a small molecular space (high density of relaxivity). Moreover, $[bpy(DTTA)_2]^{8-}$, being an ideal ligand for specific complexation of Fe^{II}/Ru^{II} and Gd^{III}, opens new perspectives for the construction of larger-sized metallodendrimeric edifices loaded with Gd^{III} on the surface.

Experimental Section

The synthesis of the ligand $H_8bpy(DTTA)_2$ has been described in the preliminary communication.[20]

Sample preparation: $[Gd_2bpy(DTTA)_2(H_2O)_4]^{2-}$ was prepared by adding solid ligand to a solution of $GdCl_3$ in a 1:2 molar ratio (pH 6.0; 50 mM MES (2-morpholinoethanesulfonic acid) buffer). A slight excess of the ligand was used (2%) and the absence of free metal ions was verified by performing a xylenol orange test.

All manipulations of the metallostar were carried out under the exclusion of oxygen to avoid oxidation of Fe^{II}. $\{Fe[Gd_2bpy(DTTA)_2(H_2O)_4]_3\}^{4-}$ was prepared by mixing a solution of $[Gd_2bpy(DTTA)_2(H_2O)_4]^{2-}$ with a freshly prepared solution of Fe^{II} ions $(Fe(NH_4)_2(SO_4)\cdot 6H_2O)$ in a 3:1 molar ratio (pH 6.0; 5 mM MES). ^{17}O-enriched water (Irakli Gverdtsiteli Research and Technology Center on High Technologies of Isotopes and Super Pure Materials LDA; ^{17}O: 10.5%) was added to the samples for ^{17}O NMR measurements to improve the sensitivity.

Potentiometry: A stock solution of Zn^{2+} (135 mM) was prepared from the chloride salt in doubly-distilled water. A stock solution of Gd^{3+} was prepared by dissolving Gd_2O_3 in a slight excess of concentrated HCl in doubly-distilled water. The excess HCl was then evaporated off. Both stock solutions were standardized by complexometric titration with Na_2H_2EDTA using xylenol orange as an indicator.

The ligand and metallostar protonation constants and the stability constants of the complexes were determined at constant ionic strength (0.1 M $(CH_3)_4NCl$). The titrations were carried out in a thermostatted vessel (25±0.2 °C) using $(CH_3)_4NOH$ as titrant solution, which was added by means of a Metrohm Dosimat 665 automatic burette. A combined glass electrode (C14/02-SC, Ag/AgCl reference electrode in 3 M KCl; Moeller Scientific Glass Instruments, Switzerland) connected to a Metrohm 692 pH/ion-meter was used to measure pH. The titrated solution (3 mL) was stirred magnetically and a constant N_2 flow was bubbled through it. Protonation and stability constants were determined at 0.002–0.003 M ligand concentrations from two or three parallel titrations. The hydrogen ion concentration was calculated from the measured pH values using the cor-

rection method suggested by Irving.[46] All protonation and stability constants were computed with the program PSEQUAD.[47]

^{17}O NMR measurements: Variable-temperature ^{17}O NMR measurements were performed on Bruker DPX-400 (9.4 T, 54.2 MHz) and Bruker Avance-200 (4.7 T, 27.1 MHz) spectrometers. A Bruker VT-1000 temperature control unit was used to stabilize the temperature, which was measured by a substitution technique. The samples were sealed in glass spheres adapted for 10 mm NMR tubes to avoid susceptibility corrections to the chemical shifts.[48] Longitudinal relaxation rates $1/T_1$ were obtained by the inversion recovery method and transverse relaxation rates $1/T_2$ by the Carr–Purcell–Meiboom–Gill spin-echo technique. Acidified water ($HClO_4$, pH 3.71) was used as an external reference. The concentrations of the solutions used were $[Gd_2bpy(DTTA)_2(H_2O)_4]^{2-}$: 0.0300 mol kg^{-1}; $\{Fe[Gd_2bpy(DTTA)_2(H_2O)_4]_3\}^{4-}$: 0.0271 mol kg^{-1}.

NMRD: The $1/T_1$ NMRD profiles were obtained at 278.0 K, 298.0 K, and 310.0 K on a Stelar Spinmaster fast field cycling NMR relaxometer (B = 2.35×10^{-4}–0.47 T; proton Larmor frequencies 0.01–20 MHz), on Bruker Minispecs (30, 40, and 60 MHz), and on Bruker spectrometers (50, 100, 200, 400, and 600 MHz). The concentrations of the samples were $[Gd_2bpy(DTTA)_2(H_2O)_4]^{2-}$: 0.500 mM; $\{Fe[Gd_2bpy(DTTA)_2(H_2O)_4]_3\}^{4-}$: 0.167 mM.

Molecular modeling: To assess the volume of $\{Fe[Gd_2bpy(DTTA)_2(H_2O)_4]_3\}^{4-}$ and the distance between the Gd^{3+} ions, a molecular model was built using the CAChe program.[49] The structure of an Sr^{2+} complex, instead of the Gd^{3+} complex, was partially optimized by means of molecular mechanics (MM2 force field) and semiempirical quantum calculations (PM5 method).

Data analysis: Simultaneous least-squares fitting of the ^{17}O NMR and NMRD data was performed by means of the programs VISUALISEUR/OPTIMISEUR on a Matlab platform, version 6.5.[50]

Relaxivity measurements on the metallostar in mouse serum and PBS: Relaxivity measurements on $\{Fe[Gd_2bpy(DTTA)_2(H_2O)_4]_3\}^{4-}$ in the presence of mouse serum and in phosphate-buffered saline (PBS; pH 7.4) were made on a Bruker Minispec 40 MHz. A solution of $\{Fe[Gd_2bpy(DTTA)_2(H_2O)_4]_3\}^{4-}$ (0.4 mM) was prepared under N_2 and the pH was adjusted to 7.4 by the addition of HCl and NaOH (both 0.1 M). Mouse serum was purchased commercially (Aldrich S-7273) and was used without further purification. Samples were incubated at 37 °C.

^{1}H NMR measurements: All spectra were recorded on a Bruker DPX-400 spectrometer (9.4 T). pH values were calculated from the equation pD = pH + 0.4.[51] The water peak was used as an internal reference (δ = 4.8 ppm).

Acknowledgements

Robert Ruloff is acknowledged for substantial contribution to the design of the ligand. This research was financially supported by the Swiss National Science Foundation and the Office for Education and Science (OFES); it was carried out within the framework of the EC COST Action D18 and the European-funded EMIL programme (LSHC - 2004–503569).

[1] R. B. Lauffer, *Chem. Rev.* **1987**, *87*, 901.
[2] P. Caravan, J. J. Ellison, T. J. McMurry, R. B. Lauffer, *Chem. Rev.* **1999**, *99*, 2293.
[3] *The Chemistry of Contrast Agents in Medical Magnetic Resonance Imaging*, (Eds.: É. Tóth, A. E. Merbach), Wiley, Chichester, **2001**.
[4] É. Tóth, L. Helm, A. E. Merbach "Relaxivity of Gadolinium(III) Complexes: Theory and Mechanism", in *The Chemistry of Contrast Agents in Medical Magnetic Resonance Imaging* (Eds.: É. Tóth, A. E. Merbach), Wiley, Chichester, **2001**, p. 45.
[5] T.-H. Cheng, Y.-M. Wang, K.-T. Lin, G.-C. Liu, *Dalton Trans.* **2001**, 3357.
[6] R. Ruloff, É. Tóth, R. Scopelliti, R. Tripier, H. Handel, A. E. Merbach, *Chem. Commun.* **2002**, *22*, 2630.
[7] S. Laus, R. Ruloff, É. Tóth, A. E. Merbach, C *hem. Eur. J.* **2003**, *9*, 3555.
[8] Z. Jászberényi, A. Sour, É. Tóth, M. Benmelouka, A. E. Merbach, *Dalton Trans.* **2005**, 2713.
[9] S. M. Cohen, J. Xu, E. Radkov, K. N. Raymond, M. Botta, A. Barge, S. Aime, *Inorg. Chem.* **2000**, *39*, 5747.
[10] G. M. Nicolle, É. Tóth, H. Schmitt-Willich, B. Radüchel, A. E. Merbach, *Chem. Eur. J.* **2002**, *8*, 1040.
[11] S. Laus, A. Sour, R. Ruloff, É. Tóth, A. E. Merbach, *Chem. Eur. J.* **2005**, *11*, 3064.
[12] G. M. Nicolle, É. Tóth, K. P. Eisenwiener, H. R. Mäcke, A. E. Merbach, *J. Biol. Inorg. Chem.* **2002**, *7*, 757.
[13] S. Torres, J. P. André, J. A. Martins, C. F. G. C. Geraldes, A. E. Merbach, É. Tóth, *Chem. Eur. J.* **2005**, in press.
[14] É. Tóth, L. Helm, K. E. Kellar, A. E. Merbach, *Chem. Eur. J.* **1999**, *5*, 1202.
[15] F. A. Dunand, É. Tóth, R. Hollister, A. E. Merbach, *J. Biol. Inorg. Chem.* **2001**, *6*, 247.
[16] a) G. Lipari, S. Szabo, *J. Am. Chem. Soc.* **1992**, *114*, 4546; b) G. Lipari, S. Szabo, *J. Am. Chem. Soc.* **1992**, *114*, 4559.
[17] V. Comblin, D. Gilsoul, M. Hermann, V. Humblet, V. Jacques, M. Mesbahi, C. Sauvage, J. F. Desreux, *Coord. Chem. Rev.* **1999**, *185–186*, 451.
[18] R. Ruloff, G. van Koten, A. E. Merbach, *Chem. Commun.* **2004**, 842.
[19] J. Costa, R. Ruloff, L. Burai, L. Helm, A. E. Merbach, *J. Am. Chem. Soc.* **2005**, *127*, 5147.
[20] a) J. B. Livramento, É. Tóth, A. Sour, A. Borel, A. E. Merbach, R. Ruloff, *Angew. Chem. Int. Ed.* **2005**, *44*, 1480; b) J. B. Livramento, É. Tóth, A. Sour, A. Borel, A. E. Merbach, R. Ruloff, *Angew. Chem.* **2005**, *117*, 1504.
[21] E. Constable, "Coordination Polymers: Discrete Systems", in *Comprehensive Coordination Chemistry II*, Elsevier, Oxford, **2004**, p. 263.
[22] a) R. Ruloff, R. N. Muller, D. Pubanz, A. E. Merbach, *Inorg. Chim. Acta* **1998**, *275–276*, 15; b) R. Ruloff, T. Gelbrich, J. Sieler, E. Hoyer, L. Beyer, *Z. Naturforsch. B* **1997**, *52*, 805.
[23] P. Letkemann, A. E. Martell, *Inorg. Chem.* **1979**, *18*, 1284.
[24] Y.-M. Wang, C.-H. Lee, G.-C. Liu, R.-S. Sheu, *J. Chem. Soc. Dalton Trans.* **1998**, 4113.
[25] G. Anderegg, *Helv. Chim. Acta* **1963**, *46*, 2397.
[26] IUPAC Stability Constants 1.05, Academic Software and K. J. Powell, Yorks, **1999**.
[27] E. Brücher, A. D. Sherry, "Stability and Toxicity of Contrast Agents", in *The Chemistry of Contrast Agents in Medical Magnetic Resonance Imaging* (Eds.: É. Tóth, A. E. Merbach), Wiley, Chichester, **2001**, p. 243.
[28] R. Ruloff, K. Arnold, L. Beyer, F. Dietze, W. Gründer, M. Wagner, E. Hoyer, *Z. Anorg. Allg. Chem.* **1995**, *621*, 807.
[29] C. Paul-Roth, K. J. N. Raymond, *Inorg. Chem.* **1995**, *34*, 1408.
[30] J. Costa, personal communication.
[31] D. H. Powell, O. M. N. Dhubhghaill, D. Pubanz, L. Helm, Y. S. Lebedev, W. Schlaepfer, A. E. Merbach, *J. Am. Chem. Soc.* **1996**, *118*, 9333.
[32] a) S. Rast, P. H. Fries, E. Belozirsky, *J. Chem. Phys.* **2000**, *113*, 8724; b) S. Rast, A. Borel, L. Helm, E. Belozirsky, P. H. Fries, A. E. Merbach, *J. Am. Chem. Soc.* **2001**, *123*, 2637.
[33] M.-R. Spirlet, J. Rebizant, J. F. Desreux, M.-F. Loncin, *Inorg. Chem.* **1984**, *23*, 359.
[34] J. J. Stezowski, J. L. Hoard, *Isr. J. Chem.* **1984**, *24*, 323.
[35] A. M. Raitsimring, A. V. Astashkin, D. Baute, D. Goldfarb, P. Caravan, *J. Phys. Chem. A* **2004**, *108*, 7318.
[36] A. V. Astashkin, A. M. Raitsimring, P. Caravan, *J. Phys. Chem. A* **2004**, *108*, 1990.
[37] F. Dunand, A. Borel, A. E. Merbach, *J. Am. Chem. Soc.* **2002**, *124*, 710.
[38] F. Yerly, K. I. Hardcastle, L. Helm, S. Aime, M. Botta, A. E. Merbach, *Chem. Eur. J.* **2002**, *8*, 1031.

[39] J. Costa, É. Tóth, L. Helm, A. E. Merbach, *Inorg. Chem.* **2005**, *44*, 4747.
[40] R. Ruloff, T. Gelbrich, J. Sieler, E. Hoyer, L. Beyer, *Z. Naturforsch. B.* **1997**, *52*, 805.
[41] a) W. D. J. Horrocks, D. R. Sudnick, *J. Am. Chem. Soc.* **1979**, *101*, 334; b) D. Parker, J. A. G. Williams, *J. Chem. Soc. Dalton Trans.* **1996**, 3613; c) A. Beeby, I. M. Clarkson, R. S. Dickins, S. Faulkner, D. Parker, L. Royle, A. S. de Sousa, J. A. G. Williams, M. Woods, *J. Chem. Soc. Perkin Trans. 2* **1999**, 493; d) R. M. Supkowski, W. D. J. Horrocks, *Inorg. Chim. Acta* **2002**, *340*, 44.
[42] M. C. Alpoim, M. A. Urbano, C. F. G. C. Geraldes, J. A. Peters, *J. Chem. Soc. Dalton Trans.* **1992**, 463.
[43] L. H. Bryant, Jr., M. W. Brechbiel, M. W. Wu, C. Bulte, J. W. Chuanchu, J. W. M. Bulte, V. Herynek, J. A. V. Frank, *J. Mater. Chem. J. Magn. Reson. Imaging* **1999**, *9*, 348.
[44] L. Burai, V. Hietapelto, R. Király, É. Tóth, E. Brücher, *Magn. Reson. Med.* **1997**, *38*, 146.
[45] P. M. May, P. W. Linder, D. R. Williams, *J. Chem. Soc. Dalton Trans.* **1977**, *6*, 588.
[46] H. Irving, M. G. Miles, L. Pettit, *Anal. Chim. Acta* **1967**, *38*, 475.
[47] L. Zékány, I. Nagypál, in *Computational Methods for Determination of Formation Constants* (Ed.: D. J. Leggett), Plenum, New York, **1985**, p. 291.
[48] A. D. Hugi, L. Helm, A. E. Merbach, *Helv. Chim. Acta* **1985**, *68*, 508.
[49] Fujitsu, *CAChe Worksystem Pro 6.1*, 2000–2003.
[50] F. Yerly, VISUALISEUR 2.3.4, OPTIMISEUR 2.3.4, Université de Lausanne, Switzerland, **1999**.
[51] K. Mikkelsen, S. O. Nielsen, *J. Phys. Chem.* **1960**, *64*, 632.
[52] L. Vander Elst, F. Maton, S. Laurent, F. Seghi, F. Chapelle, R. N. Muller, *Magn. Reson. Med.* **1997**, *38*, 604.
[53] L. D. Margerum, B. K. Campion, M. Koo, N. Shargill, J.-J. Lai, A. Marumoto, P. C. Sontum, *J. Alloys Compd.* **1997**, *249*, 185.

Received: August 9, 2005
Published online: November 28, 2005

